Title
REACTIONS OF ACTIVATED BENZO(A)PYRENE WITH DNA AND RNA

Author
Gamper, H.

Publication Date
1977-05-01

Submitted to Journal of Polycyclic Hydrocarbons and Cancer: Chemistry, Molecular Biology and Environment

REACTIONS OF ACTIVATED BENZO(A)PYRENE WITH DNA AND RNA

Howard Gamper, Thomas Meehan, Kenneth Straub, Agatha S.-C. Tung, and Melvin Calvin

May 1977

Prepared for the U. S. Energy Research and Development Administration under Contract W-7405-ENG-48

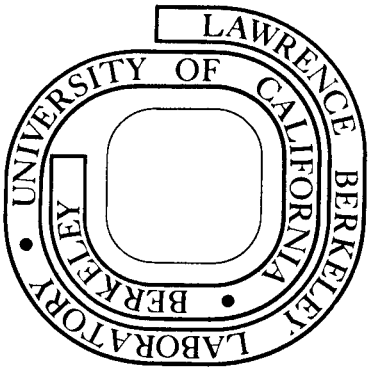

DISCLAIMER

Gamper, et al

REACTIONS OF ACTIVATED BaP WITH DNA AND RNA

ABSTRACT

The in vitro reaction of syn and anti-diol epoxides and enzyme-activated benzo[a]pyrene with DNA has been investigated. The HPLC elution profile of the anti-diol epoxide adducts closely resembles that obtained for the enzyme-activated benzo[a]pyrene adducts. High resolution mass spectroscopy of the major anti-diol epoxide adduct is consistent with a structure involving deoxyguanosine attached to the hydrocarbon via the N^2-exocyclic amine.

In addition to adduct formation, gel electrophoresis and electron microscopy demonstrate fragmentation of DNA and RNA by the synthetic diol epoxides. It is postulated that the formation of unstable phosphotriesters leads to strand scission. This reaction pathway represents a minor percentage of the total DNA modification by diol epoxide.

To be published in:

POLYCYCLIC HYDROCARBONS AND CANCER: CHEMISTRY, MOLECULAR BIOLOGY AND ENVIRONMENT

P.O.P. Ts'o and H. V. Gelboin, eds.
Academic Press

REACTIONS OF ACTIVATED BENZO[a]PYRENE WITH DNA AND RNA.

Howard Gamper, Thomas Meehan, Kenneth Straub,
Agatha S.-C. Tung, and Melvin Calvin

Chemical carcinogens are known to undergo binding in vivo to cellular macromolecules, including DNA, RNA, and protein. Covalent binding correlates with both the mutagenicity and carcinogenic activity of these chemicals, and it is this interaction with cellular macromolecules that is thought to be essential to the transformation process (Brookes and Lawley, 1964; Miller and Miller, 1974; Heidelberger, 1975). We have been investigating the binding of the widespread carcinogen BaP to model nucleic acids and calf thymus DNA under in vitro conditions.

Previous studies by ourselves and by other investigators have implicated the 7,8,9,10-positions of BaP as being involved in microsomal enzyme-mediated binding to nucleic acids. Figure 1 shows the spectral correlations between material derived from the reaction of BaP, microsomal enzymes, and poly(G) with that of synthetic 10-hydroxy-7,8,9,10-tetrahydrobenzo[a]pyrene. The similarities in both excitation and emission spectra are readily apparent. These results together with published metabolism studies suggested that the 7,8-diol-9,10-epoxide of BaP was the activated species involved in covalent binding to poly(G) and DNA (Sims et al., 1974; Meehan et al., 1976 a and b; Yang et al., 1976; Weinstein et al., 1976; Koreeda et al., 1976). We therefore undertook the synthesis of the isomeric diol epoxides of BaP using published

---

Abbreviations: BaP, benzo[a]pyrene; anti-diol epoxide, 7β,8α-dihydroxy-9α,10α-epoxy-7,8,9,10-tetrahydrobenzo[a]pyrene; syn-diol epoxide, 7β,8α-dihydroxy-9β,10β-epoxy-7,8,9,10-tetrahydrobenzo[a]pyrene; HPLC, high pressure liquid chromatography.

procedures (McCaustland and Engel, 1975; Yagi et al., 1975) and studied the binding of these compounds to poly(G), DNA, and guanosine-5'-monophosphate. We then compared the spectral and chromatographic properties of these adducts with those obtained between enzymatically activated BaP and DNA. Figure 2 shows the methodology involved in isolating monomeric adducts derived from the reaction of the diol epoxides or enzyme-activated BaP with poly(G), DNA, or 5'-GMP. The fluorescence excitation and emission spectra of the major products of these reactions are shown in figure 3. In all cases the characteristic 7,8,9,10-tetrahydrobenzo[a]pyrene spectrum was exhibited. The adducts derived from poly(G) and DNA were found to be stable compounds, whereas the 5'-GMP adduct readily underwent hydrolysis to 5'-GMP and 7,8,9,10-tetrahydroxy-7,8,9,10-tetrahydrobenzo[a]pyrene. This suggested that the latter adduct involved reaction between the 5'-phosphate and diol-epoxide, and was our first indication that multiple reaction sites in the nucleic acid (including the phosphodiester groups) could be involved in covalent binding with the hydrocarbon.

The Sephadex LH-20 column elution profile of the products derived from microsome-activated BaP and DNA is presented in figure 4. The material contained in peak Ia was concentrated and then analyzed by high pressure liquid chromatography. A similar procedure was used in analyzing the products obtained by reacting DNA with the two isomeric diol epoxides of BaP. Figures 5a and 5b show the HPLC elution profile of the diol epoxide-DNA adducts, and figure 6a shows the microsome-activated BaP-DNA product. The similarity between the elution profile of the anti-diol epoxide/DNA adducts and the microsome-activated BaP/DNA products is apparent. This was confirmed by co-injection of the two samples as shown in figure 6b. The main fluorescent peak of the anti-diol epoxide/DNA product co-chromatographs with the major enzyme-activated [G-^{3}H]BaP/DNA adduct. The elution profile of the adducts obtained from the syn-diol epoxide is markedly different from that of the enzyme-activated BaP/DNA

and anti-diol epoxide/DNA products. Thus the major products obtained in the enzyme system appear to be derived from anti-diol epoxide, although some of the minor products do co-elute in the same region as the syn-diol epoxide adducts. We have recently obtained a high resolution mass spectrum of the major anti-diol epoxide adduct (as the permethylated derivative) that is consistent with a structure involving deoxyguanosine attached to the hydrocarbon via the N^2-exocyclic amine of the purine. This structure is analogous to that reported by Jeffrey et al. (1976) for the adduct between anti-diol epoxide and poly(G). It is apparent that a large number of other products also appear in the elution profile of figure 5a, and the structures of these adducts are currently under investigation.

The reaction of diol epoxide with 5'-GMP suggested that the hydrocarbon might react with the phosphodiester backbone of DNA and RNA to give unstable phosphotriesters and that subsequent triester hydrolysis could lead to strand scission. To investigate this possibility superhelical ColE1 DNA was reacted with various concentrations of diol epoxide and then subjected to agarose gel electrophoresis. The resultant electrophoregram (Fig. 7) demonstrated that increasing concentrations of diol epoxide first nicked and then broke the DNA. Analysis of representative reaction mixtures by electron microscopy substantiated these results (Fig. 8). Both geometric forms of the diol epoxide exhibited comparable nicking activities (Fig. 9). Incubation of ColE1 DNA with syn or anti-diol epoxide at a hydrocarbon to DNA mononucleotide ratio of 0.5 - 1.0 generated form II relaxed DNA; this relaxation reflects approximately one nick per 6000 base pairs. The tetraol hydrolysis product of diol epoxide did not exhibit nicking activity.

The diol epoxide also degrades RNA. For example, when MS2 RNA was reacted with anti-diol epoxide at a hydrocarbon to RNA mononucleotide ratio of 5.0 the mobility of the viral RNA increased upon agarose gel electrophoresis

and the material ran as a diffuse rapidly migrating (low molecular weight) band. Since depurination strand scission is negligible in RNA, chain breaks are considered diagnostic for the presence of phosphotriesters (Shooter, 1975). Our evidence indicates that diol epoxide reacts with the phosphodiester backbone of RNA to form unstable phosphotriesters. Koreeda et al. (1976) have presented indirect evidence for reaction of syn-diol epoxide with the phosphate groups of poly(G).

Strand scission in DNA is generally assumed to occur through depurination or depyrimidination (Singer, 1975). This is a two-step process consisting of loss of an alkylated base followed by β-elimination. Phosphotriesters, once formed in DNA, are very stable since there are no sugar 2'-hydroxyl groups to catalyze their hydrolysis (Bannon and Verly, 1972). By analogy with RNA, diol epoxide probably forms phosphotriesters in DNA. We postulate that the hydrocarbon β-hydroxyl group on such triesters facilitates rapid hydrolysis with strand scission. Therefore, diol epoxide degradation of DNA can be explained by two entirely different mechanisms.

The kinetics of DNA nicking by anti-diol epoxide (Fig. 10) support the phosphotriester mechanism. At an anti-diol epoxide concentration just sufficient to relax superhelical ColE1 DNA the relaxation process was completed in under 4 h, implying a half-life for strand scission of less than 60 min. Such a short half-life is not consistent with depurination or depyrimidination strand scission. These processes proceed slowly as exemplified by the kinetics of dimethyl sulfate induced depurination strand scission of ColE1 DNA shown in Fig. 10. While it is conceivable that the N-glycosidic linkage to a specific hydrocarbon-base adduct could be rapidly cleaved to give an apurinic or apyrimidinic site, subsequent β-elimination to give strand scission is known to be a slow process under physiological conditions (Strauss et al., 1968; Rhaese and Freese, 1969). Acceleration of the rate of β-elimination

by the presence of diol epoxide or tetraol seems unlikely. We therefore suggest that phosphotriester hydrolysis by the mechanism outlined in Fig. 11 best explains the rapid nicking of DNA by diol epoxide.

The frequency of nicking vs. adduct formation has also been investigated. In ColE1 DNA we can detect approximately 50 adducts per supercoiled molecule before nicking is observed. The relative biological significance of strand scission vs. adduct formation has yet to be evaluated, although both processes probably occur in vivo.

References

Bannon, P. and Verly, W. (1972). Eur. J. Biochem. 31, 103-111.

Brooks, P. and Lawley, P.D. (1974). Nature 202, 781-784.

Heidelberger, C. (1975). Ann. Rev. Biochem. 44, 79-121.

Jeffrey, A.M., Jennette, K.W., Blobstein, S.H., Weinstein, I.B., Beland, F.A., Harver, R.G., Kasai, H., Miura, I. and Nakanishi, K. (1976). J. Amer. Chem. Soc. 98, 5714-5715.

Koreeda, M., Moore, P.D., Yagi, H., Yeh, H.J. and Jerina, D.M. (1976). J. Amer. Chem. Soc. 98, 6720-6722.

McCaustland, D.J. and Engel, J.F. (1975). Tetrahedron Lett. 30, 2549-2552.

Meehan, T., Warshawsky, D. and Calvin, M. (1976a). Proc. Natl. Acad. Sci. USA 73, 1117-1120.

Meehan, T., Straub, K. and Calvin, M. (1976b). Proc. Natl. Acad. Sci. USA 73, 1437-1441.

Miller, E.C. and Miller, J.A. (1974). In "The Molecular Biology of Cancer" (H. Busch, ed.), pp. 377-402, Academic Press, New York.

Rhaese, H.J. and Freese, E. (1969). Biochim. Biophys. Acta 190, 418-433.

Shooter, K.V. (1975). Chem.-Biol. Interact. 11, 575-588.

Sims, P., Grover, P.L., Swaisland, A., Pal, K. and Hewer, A. (1974). Nature 252, 326-327.

Singer, B. (1975). Progr. Nucleic Acid Res. Mol. Biol. 15, 219-284.

Strauss, B., Coyle, M. and Robbins, M. (1968). Cold Spring Harbor Symp. Quant. Biol. 33, 277-287.

Weinstein, I.B., Jeffrey, A.M., Jennette, K.W., Blobstein, S.H., Harvey, R.G., Harris, C., Autrup, H., Kasai, H. and Nakanishi, K. (1976) Science 93, 592-594.

Yagi, H., Hernandez, O. and Jerina, D.M. (1975). J. Amer. Chem. Soc. 97, 6881-6883.

Yang, S.K., McCourt, D.W., Roller, R. and Gelboin, H.V. (1976) Proc. Natl. Acad. Sci. USA 73, 2594-2598.

Figure Legends

Figure 1: Corrected fluorescence excitation and emission spectra of a) 10-hydroxy-7,8,9,10-tetrahydrobenzo[a]pyrene, and b) covalent adduct obtained by reacting BaP, rat liver microsomes, and poly(G). Corrected fluorescence spectra were recorded on a Perkin-Elmer Model MPF-3 Spectrophotofluorometer.

Figure 2: Protocol used in obtaining BaP-DNA adducts.

Figure 3: Corrected fluorescence excitation and emissions spectra of a) reaction product of anti-diol epoxide and guanosine-5'-monophosphate. b) covalent adduct obtained from poly(G) and microsome-activated BaP. c) covalent adduct from DNA and microsome-activated BaP.

Figure 4: Sephadex LH-20 column profile of products obtained after enzymatic hydrolysis of the reaction mixture from microsome-activated [G-^{3}H]BaP and DNA.

Figure 5: HPLC profile of a) material derived from reaction of anti-diol epoxide and DNA, isolated according to figure 2. b) material derived from reaction of syn-diol epoxide and DNA, isolated according to figure 2. HPLC was performed on a Varian Model 8500 LC, equipped with a Valco injection valve and two 3.9 mm x 30 cm Waters μ-Bondapak columns. A Schoeffel Model FS970 Fluorometer was used as detector (excitation at 248 nm, emission >390 nm).

Figure 6: HPLC profile of a) material isolated from reaction of DNA and microsome-activated [G-^{3}H]BaP. b) coinjection of material shown in figures 5a and 6a.

Figure 7: Agarose gel electrophoregram of ColE1 DNA reacted with anti-diol epoxide. Superhelical ColE1 DNA (mononucleotide conc. 32.5 μM) in 20 mM tris-HCl, pH 8.0, containing 0.5 mM EDTA and 5% (v/v) DMSO was incubated at 37° with (A) 0, (B) 0.0165, (C) 0.165, (D) 1.65, (E) 4.13, (F) 8.25, (G) 12,4, (H) 16.5, and (I) 165 μM anti-diol epoxide. After 24 h 40 μl aliquots were loaded onto a 1.4% agarose slab gel and electrophoresed at 50 V for 18 h. The gel was stained with ethidium bromide and the fluorescent DNA bands photographed through a Corning 3-69 filter. DNA forms I, II, and III correspond, respectively, to superhelical, relaxed, and linear ColE1 DNA.

Figure 8: Electron micrographs of ColE1 DNA (mononucleotide conc. 32.5 μM) reacted with (A) 0, (B) 16.5, (C) 165 μM anti-diol epoxide. The DNA was visualized with the Kleinschmidt technique using an unidirectional Pt/Pd shadow. With this technique hydrocarbon aggregates appear as small background granules.

Figure 9: Nicking of superhelical ColE1 DNA by diol epoxide. Superhelical ColE1 DNA (mononucleotide conc. 32.5 μM) was incubated with the indicated concs. of diol epoxide (closed circles) or tetraol (open circles) as described in Fig. 7 and analyzed by agarose gel

electrophoresis. The electrophoregrams were scanned with a Schoeffel model SD3000 spectrodensitometer in the reflectance mode. Fig. 9a refers to anti-diol epoxide and its tetraol hydrolysis product. Fig. 9b refers to syn-diol epoxide ant its tetraol dydrolysis product.

Figure 10: Kinetics of ColE1 DNA relaxation by anti-diol epoxide and dimethyl sulfate. Superhelical ColE1 DNA (mononucleotide conc. 32.5 μM) was reacted with 16.5 μM anti-diol epoxide (closed circles) or 530 μM dimethyl sulfate (open circles) in 20 mM tris-HCl, pH 8.0, containing 0.5 mM EDTA and 5% (v/v) DMSO at 37°. Aliquots were taken at various times for analysis by agarose gel electrophoresis.

Figure 11: Postulated mechanism of DNA strand scission by benzo[a]pyrene diol epoxides.

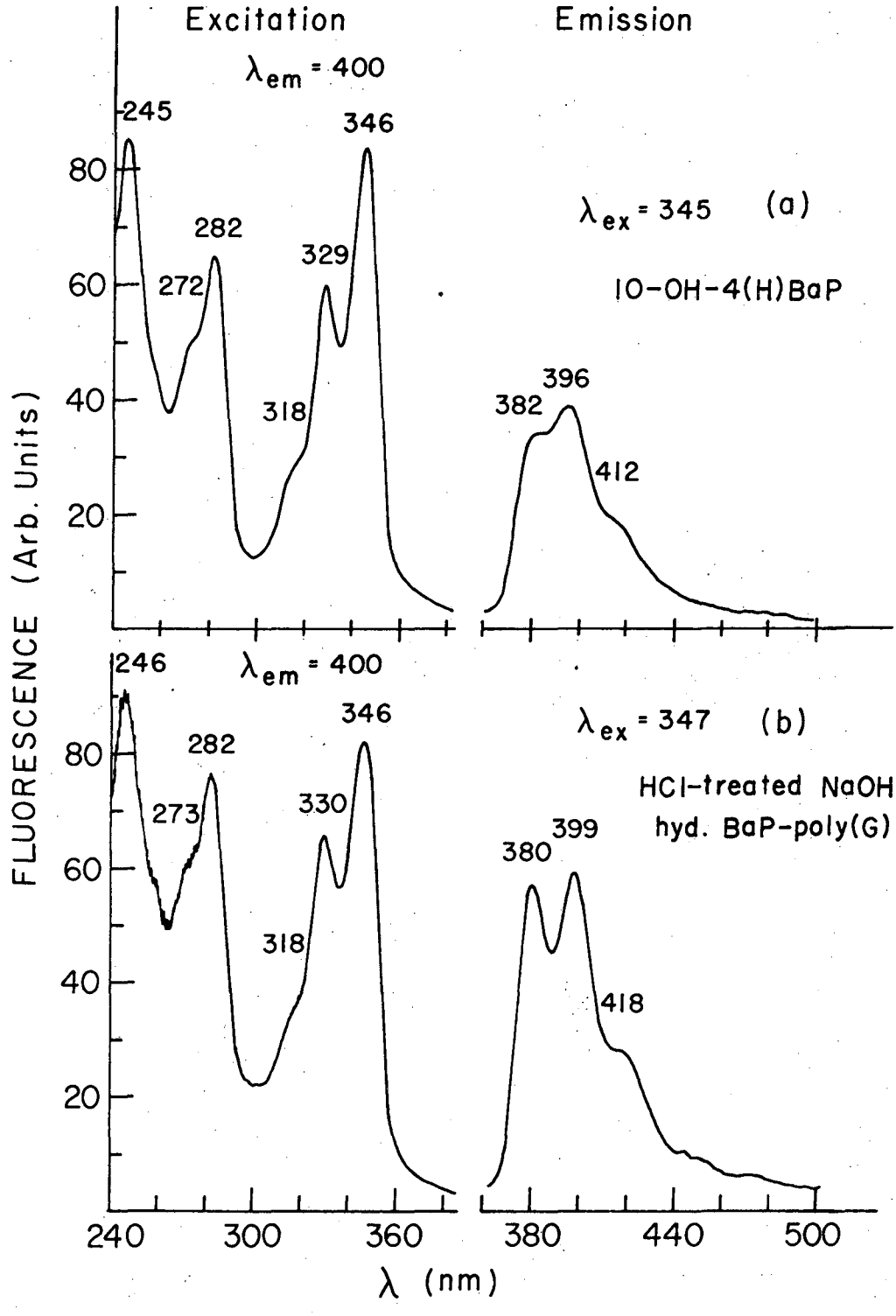

XBL7512-8789 A

Fig. 1

FORMATION OF ADDUCTS

Enzyme activation

BaP + DNA

NADPH + O_2 | rat liver (3MC induced) microsomes

BaP – DNA adduct
1HC / 40,000 bases

Chemical activation

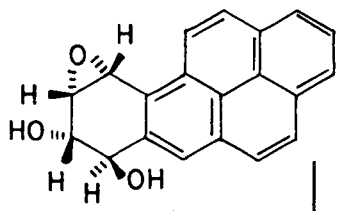

+ DNA

diol epoxide – DNA adduct

Isolation of adducts

HC – DNA

ppt EtOH | organic extraction

phosphatase | DNase phosphodiesterase

Sephadex LH – 20

HPLC

analysis of products by
1) radioactivity
2) absorbance and fluorescence spectroscopy
3) mass spectrometry

XBL771-4109

Fig. 2

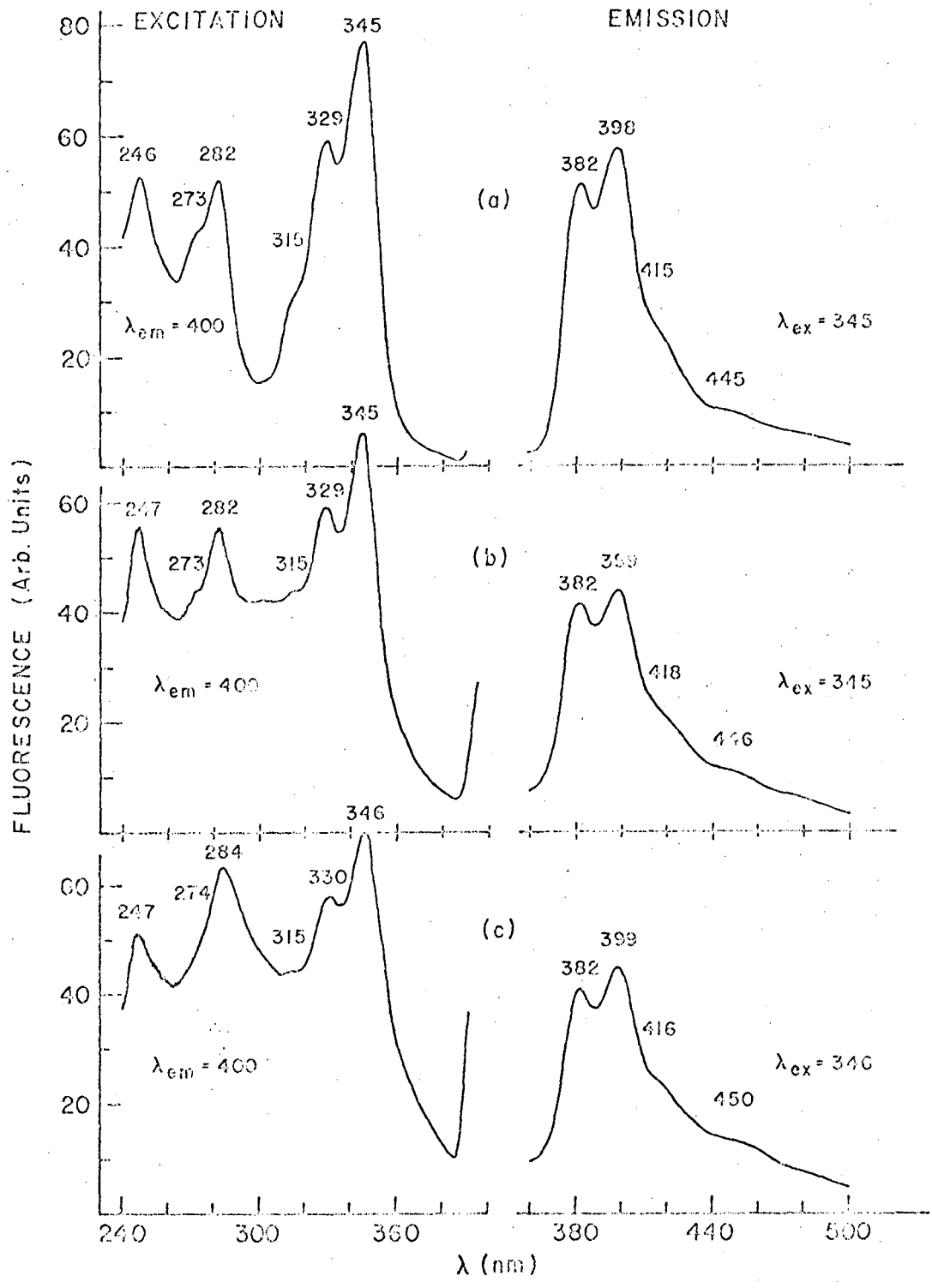
EXCITATION
EMISSION
FLUORESCENCE (Arb. Units)
λ (nm)
(a)
(b)
(c)
λem = 400
λex = 345
λex = 340
246
282
273
315
329
345
382
398
415
445
247
284
274
330
346
399
416
418
446
450
240
300
360
380
440
500
XBL 776-9143

Fig. 3

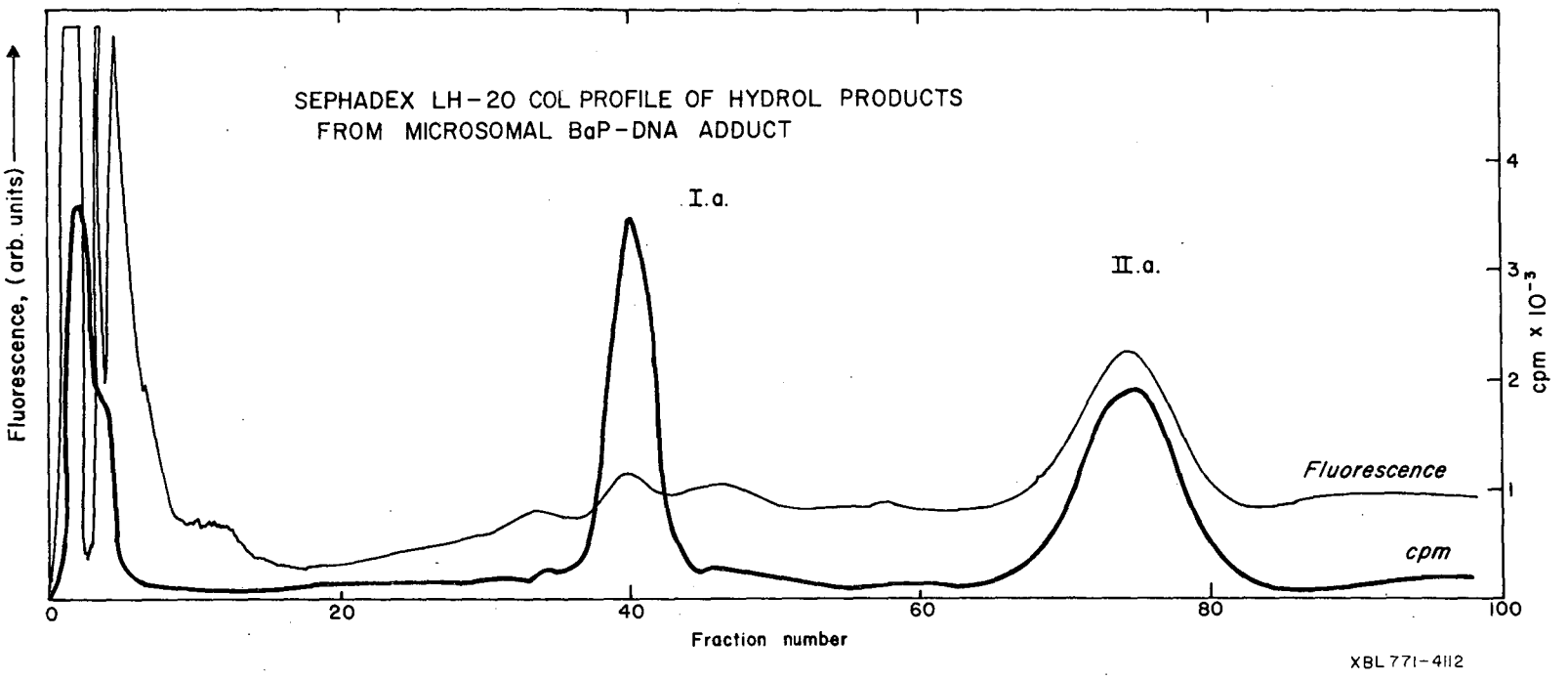
SEPHADEX LH-20 COL PROFILE OF HYDROL PRODUCTS
FROM MICROSOMAL BaP-DNA ADDUCT
I.a.
II.a.
Fluorescence
cpm
Fluorescence, (arb. units)
cpm x 10⁻³
Fraction number
0
20
40
60
80
100
1
2
3
4
XBL 771-4112

Fig. 4

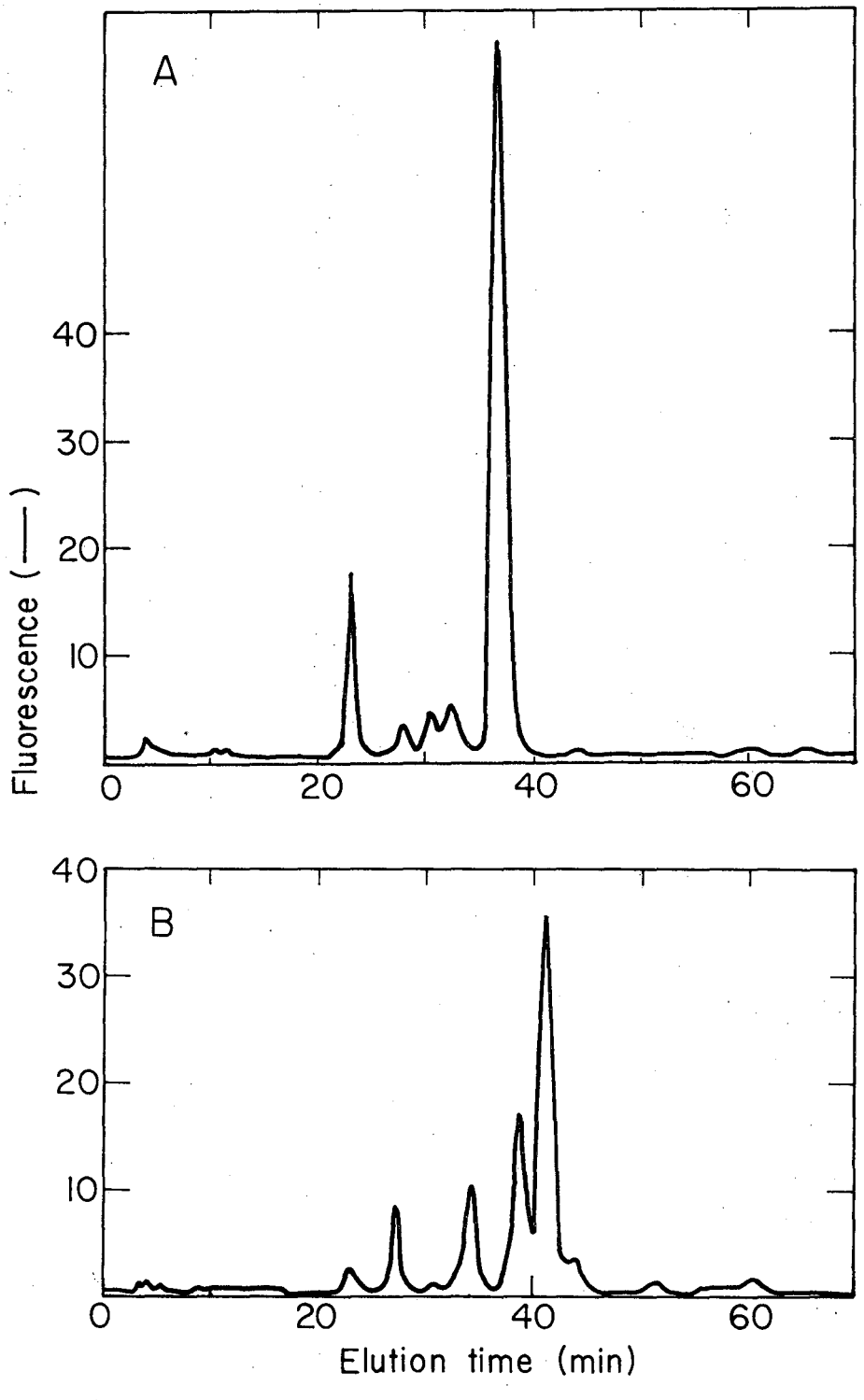

XBL 775-4378

Fig. 5

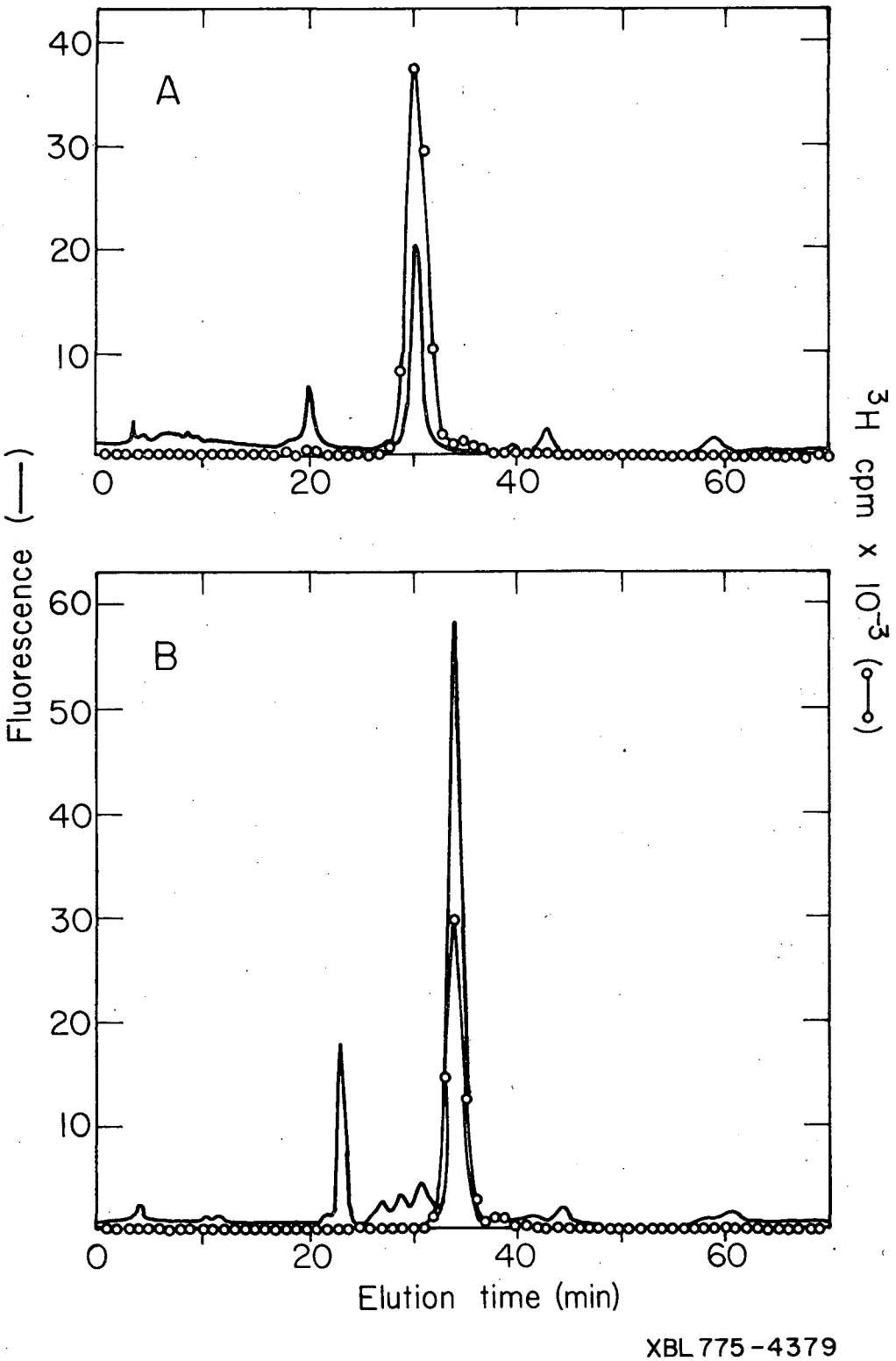
A
B
40
30
20
10
60
50
0
20
40
60
Fluorescence (—)
^{3}H cpm x 10^{-3} (o—o)
Elution time (min)
XBL 775-4379

Fig. 6

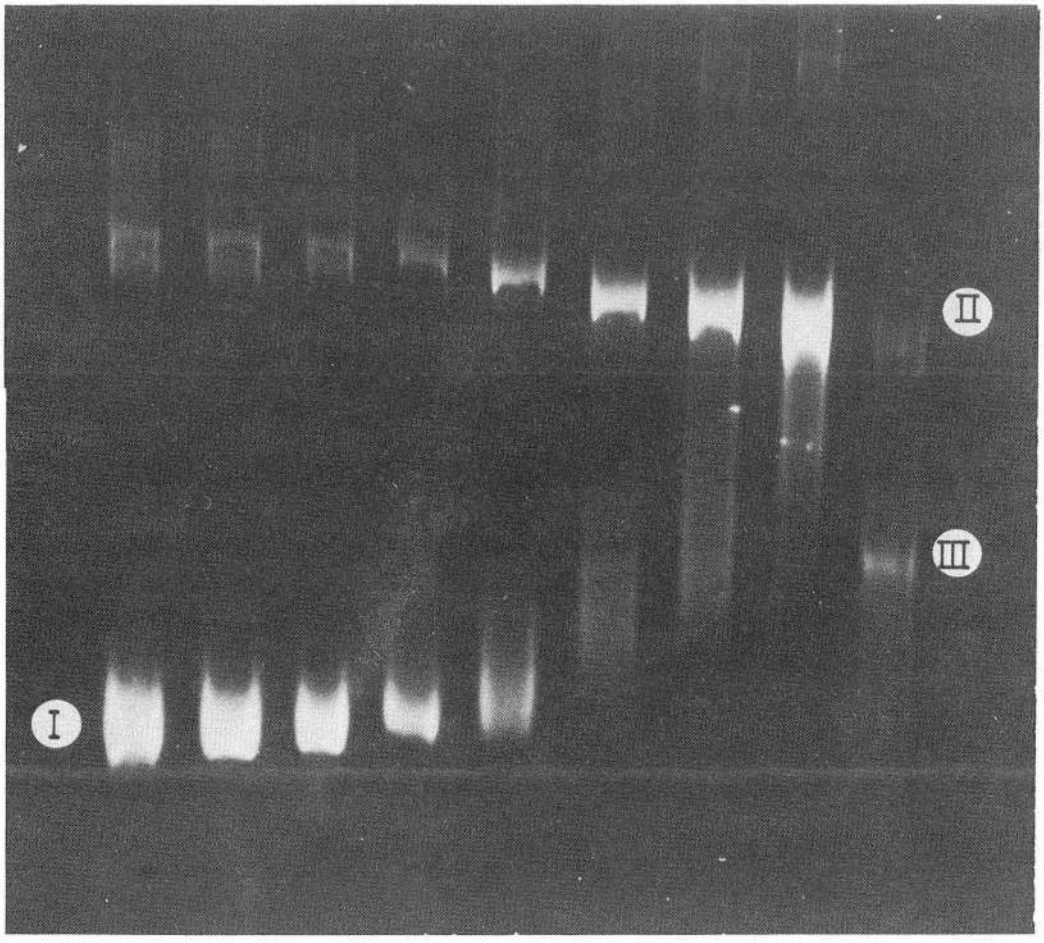

XBB 774-4155

Fig. 7

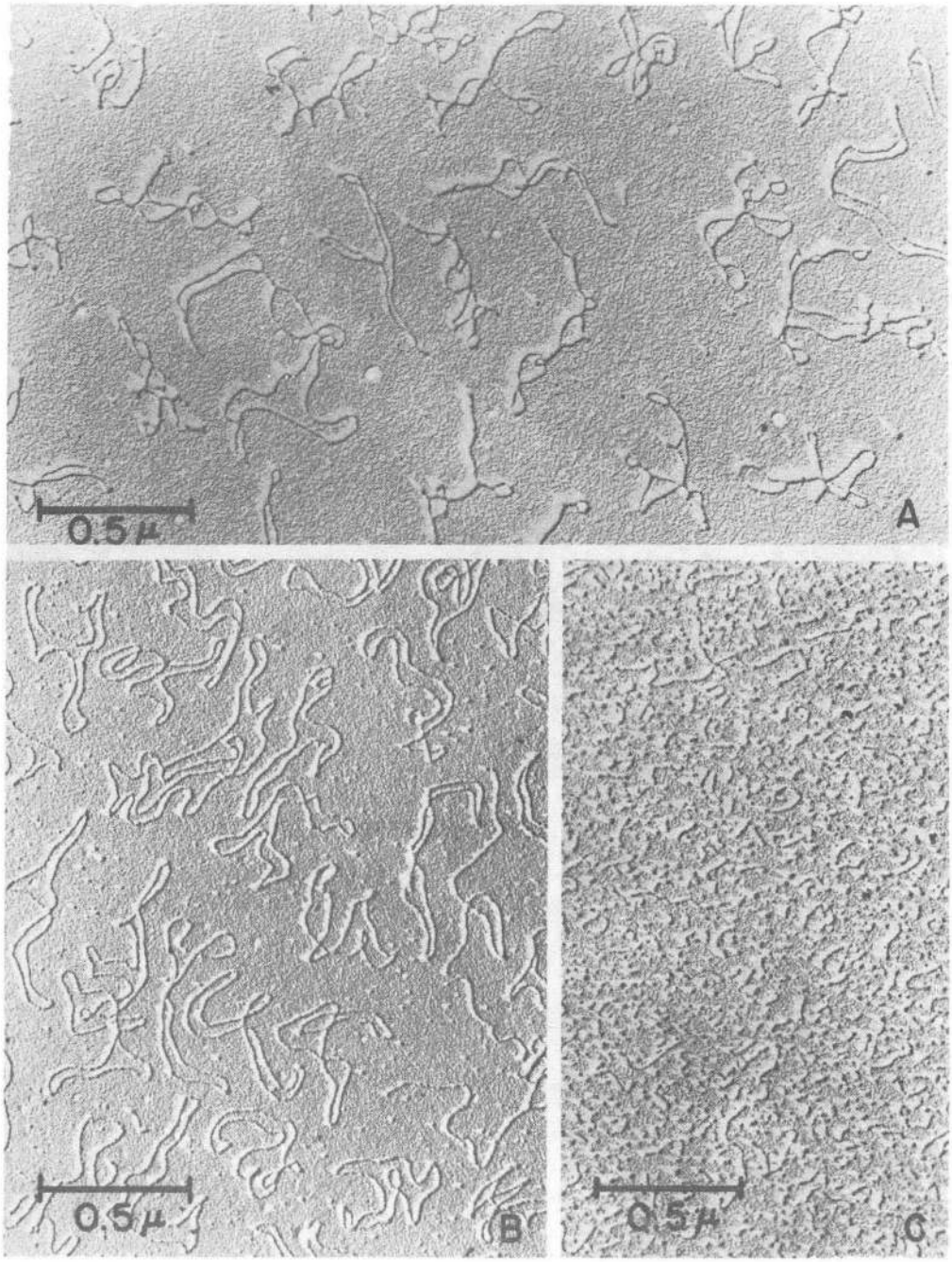

XBB 771-279

Fig. 18

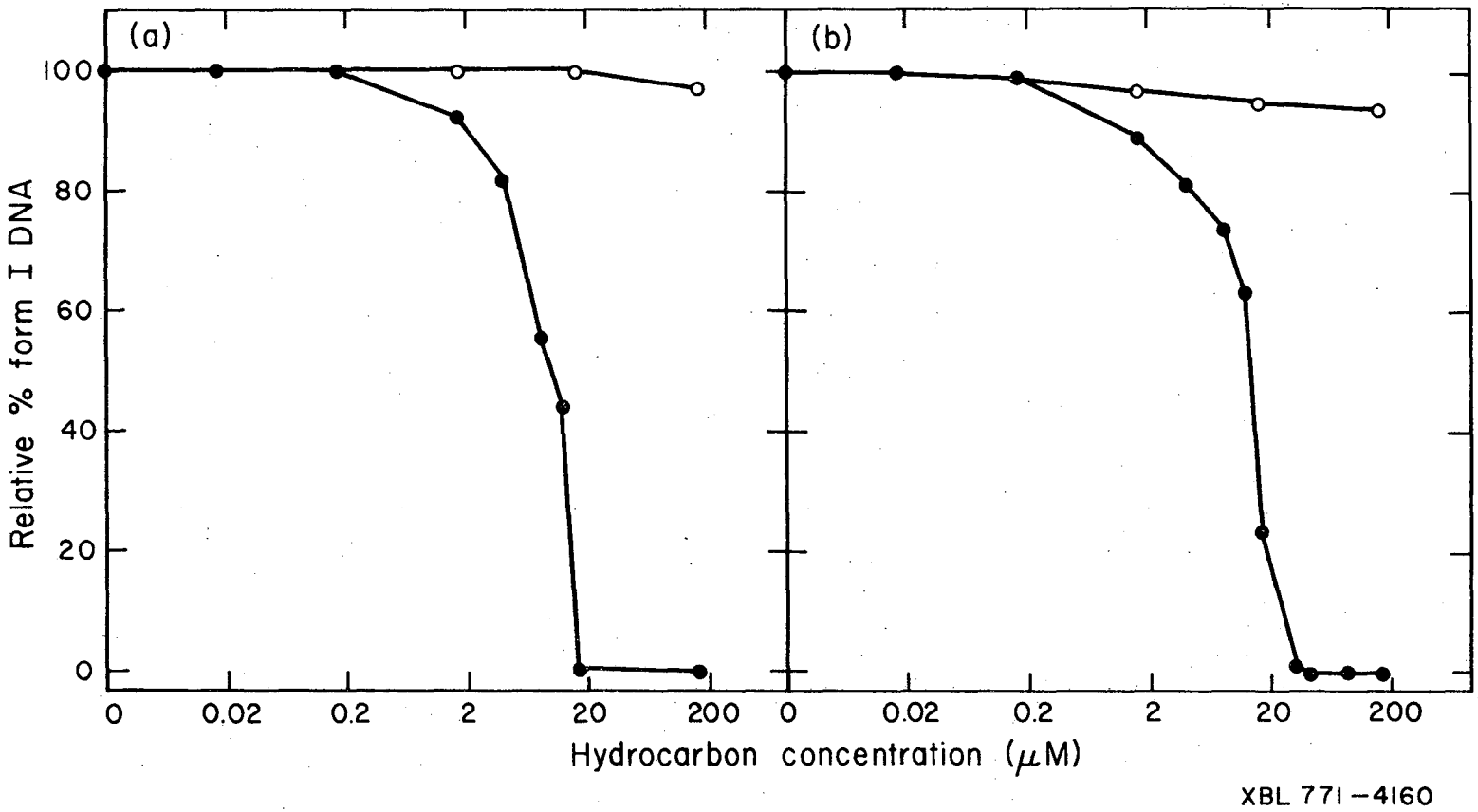

Fig. 9

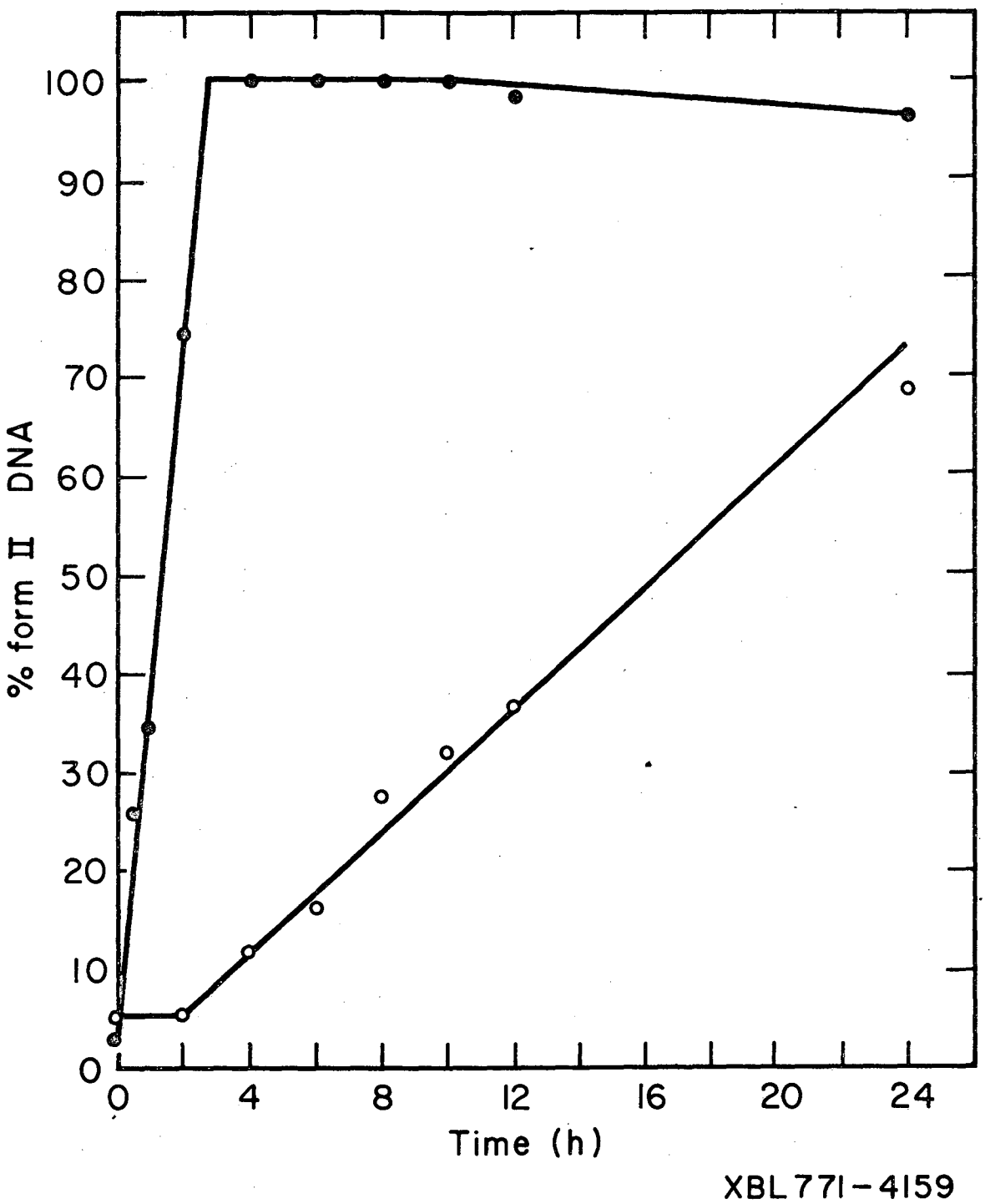
100
90
80
70
60
50
40
30
20
10
0
% form II DNA
0
4
8
12
16
20
24
Time (h)
XBL771-4159

Fig. 10

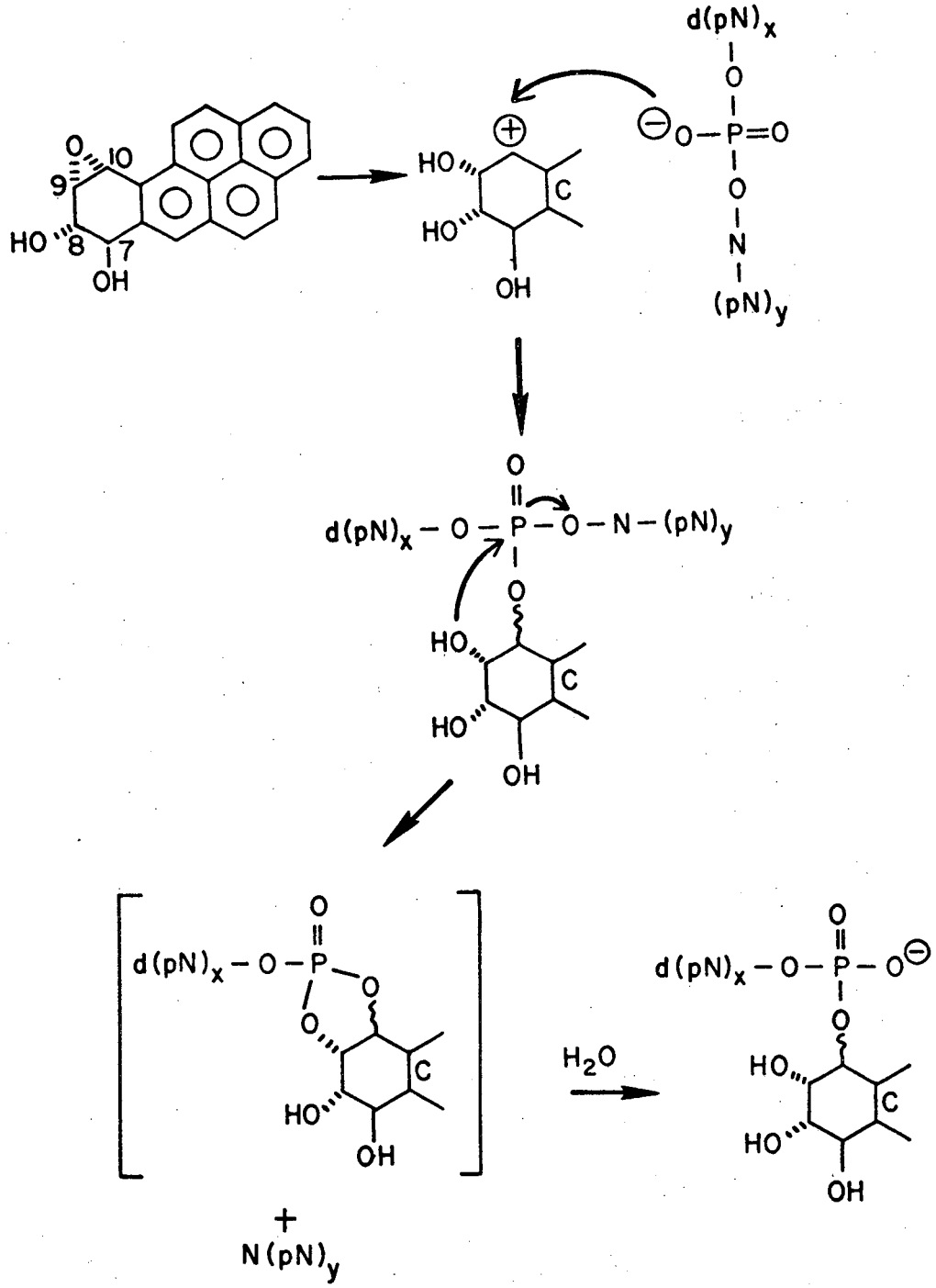

XBL771-4115A

Fig. 11

TECHNICAL INFORMATION DIVISION
LAWRENCE BERKELEY LABORATORY
UNIVERSITY OF CALIFORNIA
BERKELEY, CALIFORNIA 94720